Spatial non-stationarity in forest fire driving factors in the lowlands of Nepal: A case study of Madhesh Province

Gunjan Adhikari[1*], Nabin Kumar Yadav[2], Khagendra Prasad Joshi[3], Sandip Mahara[4], Dristee Chad[5], Damodar Gaire[6], Rajan Subedi[4,7]

[1] College of Forestry, Wildlife and Environment, Auburn University, Auburn, AL, USA
[2] Ministry of forest and environment, Madhesh Province, Janakpurdham, Nepal
[3] Kathmandu Forestry College, Kathmandu, Nepal
[4] Tribhuvan University, Institute of Forestry, Pokhara Campus, Pokhara, Nepal
[5] Department of Geography and Environmental Sustainability, University of Oklahoma, USA
[6] Tribhuvan University, Institute of Forestry, Hetauda, Nepal
[7] Arthur Temple College of Forestry and Agriculture, Stephen F. Austin State University, USA
**Corresponding author: gunjanadhikari58@gmail.com*

Abstract

Madhesh Province, located in the southern lowlands of Nepal, experiences frequent forest fires under strong human–forest interactions. Previous fire-risk studies in Nepal rarely account for spatial non-stationarity in the relationships between fire occurrence and its drivers. We aggregated VIIRS (2012–2023) active-fire detections to 136 local administrative units and modelled municipal fire counts using a Poisson generalised linear model (GLM) and a Poisson geographically weighted regression (GWR). Across the province, aspects, land surface temperature, rangeland and agricultural area, canopy height, NDVI, and road length were generally positively associated with fire counts, whereas precipitation and wind speed were negative; several land-cover and anthropogenic variables showed spatially varying effects in the GWR. The local GWR improved model fit (deviance explained = 0.994) compared with the global GLM (0.913), both trained with fire incidents from 2012-2022, and produced a more accurate prediction map (AUC = 0.825 vs 0.769, validated using 2023 fire detections). Both models indicated that ~22 per cent of Madhesh Province falls within high fire-risk zones. Overall, accounting for spatial heterogeneity improves forest-fire risk mapping in Nepal's lowlands and supports locally tailored prevention and preparedness strategies.

Keywords: Forest fires, Generalised linear model (GLM), Geographic weighted regression (GWR), Risk map, Spatial heterogeneity

INTRODUCTION

Forests play a crucial role in facilitating soil and water conservation efforts, as well as serving as regulators of climate and carbon cycles (Piao *et al.,* 2018). However, forest fires have caused significant adverse impacts on wildlife, forest ecosystems, and greenhouse gas emissions. The GFED5 database estimates global burned area of about 774 ± 63 million ha per year for 2001–2020 (Chen *et al.,* 2023; Robinne, 2021). In addition, it is anticipated that the potential risk will further escalate given the projected 2°C global temperature increases under current and future climatic conditions (Aponte *et al.*, 2016). Forest fire is one of the major factors impacting forest ecosystems in Hindu Kush region negatively (Bhattarai *et al.*, 2022). Analysing historical data in Nepal reveals that approximately

40,000 hectares of forest land are affected by fire issues each year and, that this area has been increasing over time (Bajracharya, 2002; Mishra *et al.*, 2023).

Forest fires can be attributed to a range of factors that can be broadly categorised as climatic, topographic, vegetative, and socioeconomic factors (Zhang *et al.*, 2011). It is important to note that these factors exhibit variations across different temporal and spatial scales. Climatic variables regulate the water content and forest fuel accumulation (Sharples, 2009) and have effects at larger scales than other determinants (Turco *et al.*, 2013). Forest fuels, as a primary determinant in forest fire originate from vegetation and have a direct influence on flammability (İnan *et al.*, 2017). Topography which shapes the structure and distribution of plants, plays a pivotal role in determining the likelihood, speed, and direction of forest fires *(*Maingi and Henry, 2007; *Yang et al.*, 2021). The frequency of forest fires is influenced by socioeconomic variables, as urban expansion, growing transportation networks, and human activities increase pressure on wildlands and bring potential ignition sources closer to forests (Cardille *et al.*, 2001; Kolanek *et al.*, 2021).

In recent years, advancements in technology have improved access to remotely sensed data on forest cover, bioclimatic conditions, and anthropogenic factors, thereby enabling significant research into their effects on forest fires (Matin *et al.*, 2017). Furthermore, modelling tools have been developed to analyse and visualise forest fires. However, when conducting extensive geographic studies, it is more reasonable to consider diverse relationships rather than uniform ones. For instance, Koutsias *et al.* (2010) observed a noteworthy improvement in the explanatory power of classical linear regression when incorporating varying relationships instead of constant ones in modelling fire densities. Their study, conducted at the provincial level (NUTS-3) across countries in the European Mediterranean Basin, utilised geographically weighted regression (GWR), thus pioneering the application of GWR in fire modelling studies (Martínez-Fernández *et al.*, 2013). Previous studies conducted in Nepal have primarily focused on mapping vulnerable areas prone to forest fires (Matin *et al.*, 2017; Parajuli *et al.*, 2020; Parajuli *et al.*, 2023; Adhikari *et al.*, 2025). These studies have employed various modelling approaches to examine the relationship between different drivers and the extent of forest fires (Qadir *et al.*, 2021; Mishra *et al.*, 2023; Joshi *et al.*, 2024). However, the spatial variability among these drivers has not been adequately addressed in these studies.

In Madhesh province, forest ecosystem values have increased over the past decade, indicating a high dependence of local people on forest resources in the region (Shah *et al.*, 2022). Community people depend on forest resources, like timber, fuelwood, fodder and other non-timber forest products (NTFPs), to sustain their agro-economic livelihoods, with studies indicating that poorer families rely on these resources to a greater extent (Posavec, 2023). Consequently, the subsistence livelihood of residing communities, especially the marginalised communities, is affected if these forest resources are lost or damaged. The increasing forest fires are degrading the forests in an alarming rate (Adhikari *et al.*, 2025). Despite numerous efforts to understand the drivers of forest fires, predictive models such as GLM (Joshi *et al.*, 2024), MaxEnt (Paudel *et al.*, 2024) and deep learning approaches (Mishra *et al.*, 2023; Dhakal *et al.*, 2024) often generalise these variables, thereby overlooking their spatial heterogeneity (Li *et al.*, 2022). To address this gap, we hypothesise that (i) the

relationships between forest fire occurrence and its driving factors exhibit spatial non-stationarity across Madhesh Province, and (ii) a Poisson GWR model, by explicitly accounting for spatial heterogeneity, provides improved explanatory power and model performance compared to a global Poisson generalised linear model (GLM). We therefore compare GLM and GWR results and validate the best-fitting model using ROC/AUC. The results reveal spatial patterns of forest fires and dominant local drivers, providing actionable insights for provincial and local governments to develop site-specific fire-risk management policies and precautionary measures, with potential applicability to other lowland regions of Nepal.

MATERIAL AND METHODS

Study area

The study area encompasses the entire geographical region of Madhesh Province, located between 26°23'N - 27°28'N latitude and 84°27'E - 86°54'E longitude, with an elevation range of up to 918 meters. It comprises eight districts: Parsa, Bara, Rautahat, Sarlahi, Mahottari, Dhanusha, Siraha, and Saptari. Madhesh Province is bordered by the Shiwalik hills to the north, India to the south, the Koshi river to the east, and Bagmati Pradesh to the west. Forests occupy approximately 27.29 per cent of the province's total land area, with those in the Chure region alone comprising 152,339

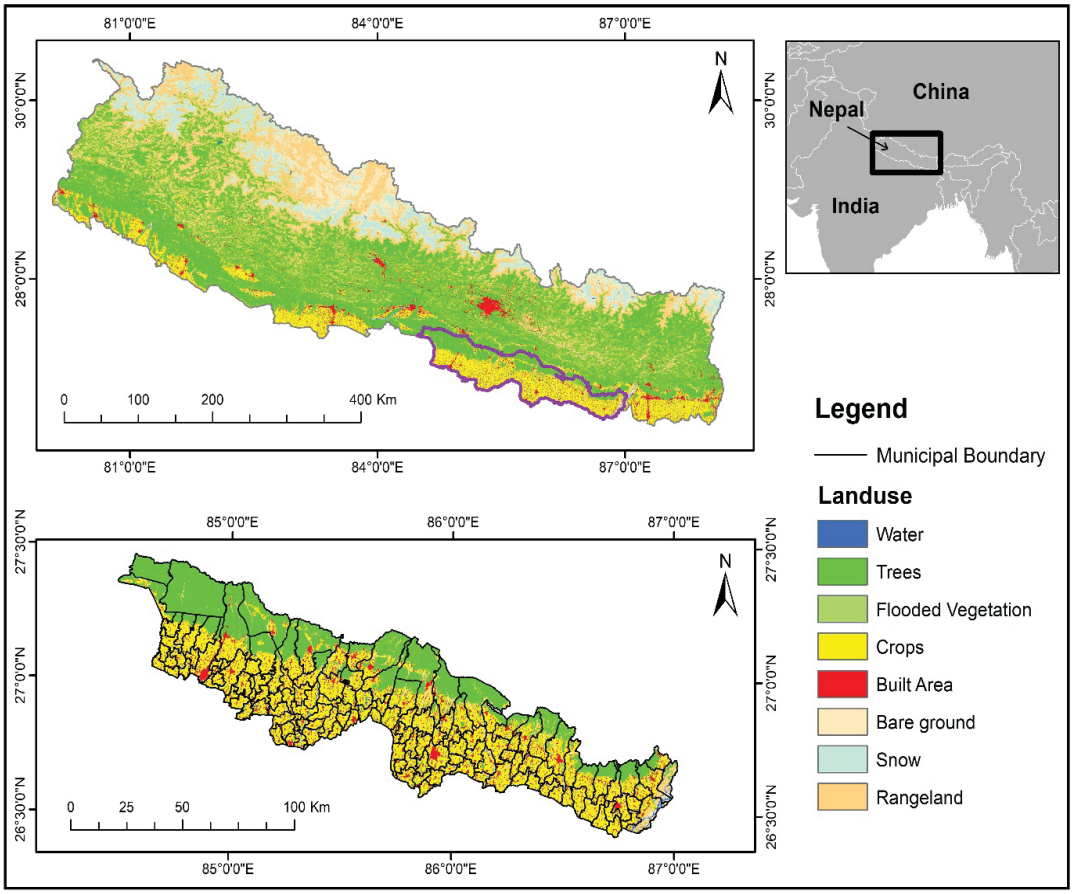

Figure 1: Study area map showing the land cover classes at the local level division within the region

hectares, of the province's total area. Most of the province, nearly 90 per cent of its land area, lies in the lower tropical climate zone, while the remaining part belongs to the upper tropical climate zone. Administratively, the province comprises 136 local units (73 municipalities, 59 rural municipalities, 3 sub-metropolitan cities, and 1 metropolitan city), all of which were used as analytical units in the regression models. In addition, three protected areas within the province, Parsa National Park, Chitwan National Park, and Koshi Tapu Wildlife Reserve, were included among the local units. The GWR method requires a minimum of 20 features for computation and achieves optimal results with larger datasets (Devkota *et al.*, 2014). The number of municipal divisions in the province meets this requirement, as shown in Figure 1.

Data acquisition and processing

The data employed in this study were classified into two categories: forest fire records spanning various time periods, and forest fire drivers selected based on existing literature, as presented in Table 1. In the modelling analysis, forest fire records served as the dependent variable, while other factors were treated as independent variables to identify the key drivers of forest fires. Predictive modelling was then applied to examine the impact of each driver at varying spatial scales.

Dependent variable (Forest fire data)

Historical fire data from the Visible Infrared Imaging Radiometer Suite (VIIRS) product for the period 2012-2023 were obtained from NASA's Fire Information for Resource Management System (FIRMS, https://firms.modaps.eosdis.nasa.gov/). The dataset contains the coordinates of the fire location, the date and time, and the confidence level. For fire incidents, the VIIRS 375m active fire data product provides the highest spatial resolution among freely available fire datasets (Sofan *et al.*, 2020) and is therefore preferred over MODIS (Moderate Resolution Imaging Spectroradiometer) due to its greater accuracy (Coskuner, 2022). Despite some limitations in detecting forest fire due to the dense canopy cover (Giglio *et al.*, 2006), this method is still frequently used for monitoring forest fire. For better accuracy, only points with high and normal confidence levels are considered in order to filter out false alarms (Giglio *et al.*, 2020). This helped eradicating potential smaller fires, which occurred mainly in agricultural area.

As for the burned area, the Terra and Aqua combined MCD64A1 monthly 500 m global gridded data was used. This technique uses 1 km MODIS active fire data combined with 500 m MODIS Surface Reflectance images (Giglio *et al.*, 2020). The data on burned areas for the years 2012-2023 were compiled and analysed using ArcGIS Pro 3.0 (ESRI, 2022) and were used to summarise inter-annual burned-area trends (Figure 3). However, they were not used as a dependent variable in the regression models.

Independent variable

The independent variables used in the study included various terrain factors, weather factors, vegetative factors, and anthropogenic factors, as indicated in Table 1. The Aster global Digital Elevation Model (DEM) with a spatial resolution of 30 meters was obtained from the USGS website (https://earthexplorer.usgs.gov/). In addition, slope and aspect were derived using the spatial analyst tool in ArcGIS Pro 3.0. For the weather factor, precipitation data for the years 2000-2018 were downloaded from

Table 1: Datasets used in the study along with relevant and their information

Variables		Data	Classes	Unit	Resolution	Year	Source
Forest fire records (Dependent variables)		2012-2023 fire incidents records (point data)	-	-	375 m	2012-2023	FIRMS/NASA
		Burnt Area (2012-2023)	-	Km^2	500m	2012-2023	MODIS (MCD64A1 monthly global grided product)
(Independent variable)	Weather factor	Land Surface Temperature	Continuous	°C	1000 m	2012-2023	LAADSDAAC/ MOD11C3
		Wind speed	Continuous	m/s	250 m	2023	Global wind atlas
		Precipitation	Continuous	mm	4500m	2000-2018	Worldclim
	Terrain factor	Slope	Continuous	°	30 m	2023	USGS Earth Explorer (ASTER GDEM v3)
		Elevation		m	30 m	2023	
		Aspect		°	30 m	2023	
	Vegetative factor	Land cover type (area)	Categorical	m	10 m	2022	ESRI 2022
		Normalised Vegetative Index (NDVI)	Continuous		10 m	2023	Copernicus sentinel 2
		Canopy Height	Continuous	m	30 m	2019	GLAD
		Above ground biomass	Continuous	Mg/ha	100 m	2020	ESA CCI Global Forest AGB
	Anthropogenic factors	Population density	Continuous	per km2	1000 m	2020	SEDAC
		Length of road	Vector	m	-	2015	Department of survey

Worldclim (Fick and Hijmans, 2017). Land Surface Temperature (LST) was derived by filtering the mean monthly values during the pre-monsoon season (March-May) of each year, using compiled MODIS Level-1 B 1-km LST HDF files for 2012-2023 obtained from NASA/MODIS and processed in ArcGIS Pro 3.0. Windspeed data were sourced from the Global Wind Atlas (https://globalwindatlas.info/), while land use type information with a spatial resolution of 10 meters was accessed from ESRI (https://livingatlas.arcgis.com/landcover/). The Level 1c format Sentinel-2A NDVI data covering May 30, 2021 to March 1, 2023, specifically for the summer period (March-May), were downloaded from the Copernicus Open Access Hub. Previous studies on forest fires in Nepal have shown that the pre-monsoon months represent the peak fire season (Parajuli *et al.*, 2020; Joshi *et al.*, 2024; Adhikari *et al.*, 2025), and we therefore used NDVI from this period to better understand its relationship with fire occurrence. NDVI was then calculated using the near-infrared (NIR) and red spectral bands as shown in the equation (1).

NDVI= (NIR-Red)/ (NIR + Red) (1)

Canopy height data was obtained from the Global Ecosystem Dynamics Investigation (GEDI) dataset available at (https://glad.umd.edu/dataset/gedi). The Above Ground Biomass dataset, generated as part of the European Space Agency's (ESA's) Climate Change Initiative (CCI) program by the Biomass CCI team, was accessed through (https://climate.esa.int/).

Forest fires are also influenced by anthropogenic factors like road networks, urban areas, and recreational areas (Ganteaume *et al.*, 2013). Therefore, population density, an anthropogenic variable, was acquired from the Socioeconomic Data and Application Center (CIESIN, 2018). Road networks were obtained from the Department of Survey through (https://opendatanepal.com/dataset), and the length of the road networks was determined using spatial join tools. Once all the variables were acquired, they were resampled to a consistent resolution of 30x30 meters using ArcGIS Pro 3.0 for spatial alignment and consistency during spatial overlay, zonal statistics, and model implementation. Next, the zonal statistics tool was used to calculate the corresponding average values from the raster datasets of all influencing drivers at the municipal level. Subsequently, the drivers were normalised using Equation (2) to account for differences in scale level among the variables. Normalisation facilitates the interpretation and comparison of coefficients by aligning all variables on a common scale, without impacting the model predictions (Zeng and Tao, 2023).

$$\chi_i = \frac{\chi - \chi_{min}}{\chi_{max} - \chi_{min}} \quad \text{..... (2)}$$

Where, Xi is the normalised value

$Xmax$ is the maximum value in dataset

$Xmin$ is the minimum value in the dataset

The Appendix Table 1 shows the variation in forest fire driving variables across the study area, highlighting the need for to apply a GWR model to better capture local patterns and dynamics.

Data Analysis

Multicollinearity test

Since not all variables may contribute equally to forest fire occurrence and some may be independent, the variance inflation factor

(VIF) was computed among variables using the Equation (3) to reduce information redundancy.

$$VIF = \frac{1}{1-R^2} \quad \text{.....(3)}$$

In this context, R^2 represents the squared multiple correlations of the independent variable when it is regressed on other independent variables. To address multicollinearity, the variables with VIF>5 were removed (Chatterjee and Hadi, 2015) sequentially (from highest value), and VIF was recalculated after each removal step until all retained variables had VIF<5 (Table 2).

Table 2: Variables selected for modelling forest fire risk. Only the variables with VIF less than 5 were selected for modelling purposes.

Variables	Abbreviation	Before	After
Elevation	E	***6.204***	
Aspect	A	1.198	1.084
Precipitation	PPT	2.021	1.793
Slope	S	***5.687***	
Wind speed	WS	1.981	1.857
Canopy height	CH	*7.515*	4.272
Area under water	AW	***5.371***	
Forest Area	AF	1.988	1.558
Agriculture Area	AA	1.845	1.753
Built-up Area	AB	1.339	1.27
Bare land area	ABL	***5.999***	
Rangeland Area	AR	3.202	1.202
Population density	PD	1.646	1.621
Above ground biomass	AGB	***7.699***	
Normalised difference vegetation index	NDVI	2.677	2.045
Land surface temperature	LST	5.01	4.47
Road length	RL	2.713	2.307

Model

We used both global (GLM) and local (GWR) models across the entire Madhesh province to compare the performance and spatial non-stationery properties of forest fire driving variables. We used incidents from 2012-2022 after filtering incidents with low confidence to reduce false detections and agricultural residue burning.

GLM is the most preferred regression analysis due to its precise prediction and estimation for non-uniform distributed data (Meyers *et al.*, 2012). It uses various types of distributions such as the binary (presence-absence) and Poisson (count). For our study, a GLM was fitted using a Poisson distribution, as it is well-suited for non-negative count data, representing count of fire occurrences in each

feature (Chen *et al.*, 2018). The following is the probability of mass function for the Poisson distribution:

$$P(Y=y) = P(Y=y) = \frac{e^{-\lambda}\lambda^{y}}{y!} \quad \text{.....(4)}$$

Where y represents count variable, and λ is both the variance and the mean, and is greater than zero. In the Poisson distribution the mean is equal to the variance and over-dispersion is when the variance is greater than mean (Mullahy, 1986; Xiao *et al.*, 2015). We used Arc GIS Pro 3.0 for GLM model selecting the Poisson distribution (ESRI, 2022). The tool uses the explanatory variables (forest fire variables) to predict the count distribution along the features.

Likewise, we employed the GWR Model, a widely discussed and utilised method in various publications (Koutsias *et al.*, 2010; Sá *et al.*, 2011). Unlike the global logistic regression model, which overlooks the spatial non-stationarity of forest fires and their causes, the GWR model exhibited enhanced prediction accuracy and a better fit (Li *et al.*, 2022). This model allowed us to examine the regression coefficients for each location, providing insights into the specific associations between fire incidences and explanatory factors within distinct regions (Koutsias *et al.*, 2010; Sá *et al.*, 2011). The general relationship of GWR is as follows (Brunsdon *et al.*, 1996):

$$y = \beta o\,(u, v) + \sum_{j=1}^{p} \beta j\,(u, v) Xj + \varepsilon \quad \text{.... (5)}$$

Where y is a dependent variable, Xj is the j th independent variable, p is the number of independent variables, ε is the remaining of model and βj is the regression coefficients that are a function of the position of observational points (u, v).

A total of 136 municipal units were used as features for local observation in the GWR model. The GWR analysis yielded several diagnostic outputs (such as standard errors, influence index, Cook's D statistics, local R^2 statistic, and local standard deviation) and parameter estimates (local coefficients for each independent variable) that were visualised within a GIS environment (Charlton and Fotheringham, 2009). A fixed bi-square kernel was selected to define spatial weights, emphasising nearby observations while limiting the influence of distant ones (Li *et al.*, 2022). Both fixed and adaptive bandwidth approaches were initially evaluated using corrected Akaike Information Criterion (AICc). Finally, the optimal bandwidth was determined using a golden search rule for obtaining the minimum AICc value, and the final model, with 30 fixed neighbours, was used for prediction in Arc GIS 3.0 (ESRI, 2022). Then we used the spatial autocorrelation (global Moran's I) tool on residuals for assessing biasness and dispersion (Comber *et al.*, 2023; Yu *et al.*, 2022). The model's performance was assessed using Receiver Operating Characteristics (ROC) curves and Area Under Curve (AUC) values which ranges from 0-1 with higher values indicating better results (Flach, 2016; Hosmer, 2013). We used 2012-2022 fire incidents for modelling, while fire occurrences in 2023 were used exclusively for validation. The ArcSDM tool was used to validate the final predicted outputs from both models using ArcGIS Pro 3.0. Finally, the outputs for the fire risk maps were prepared using the Natural Jenks method to classify risk levels.

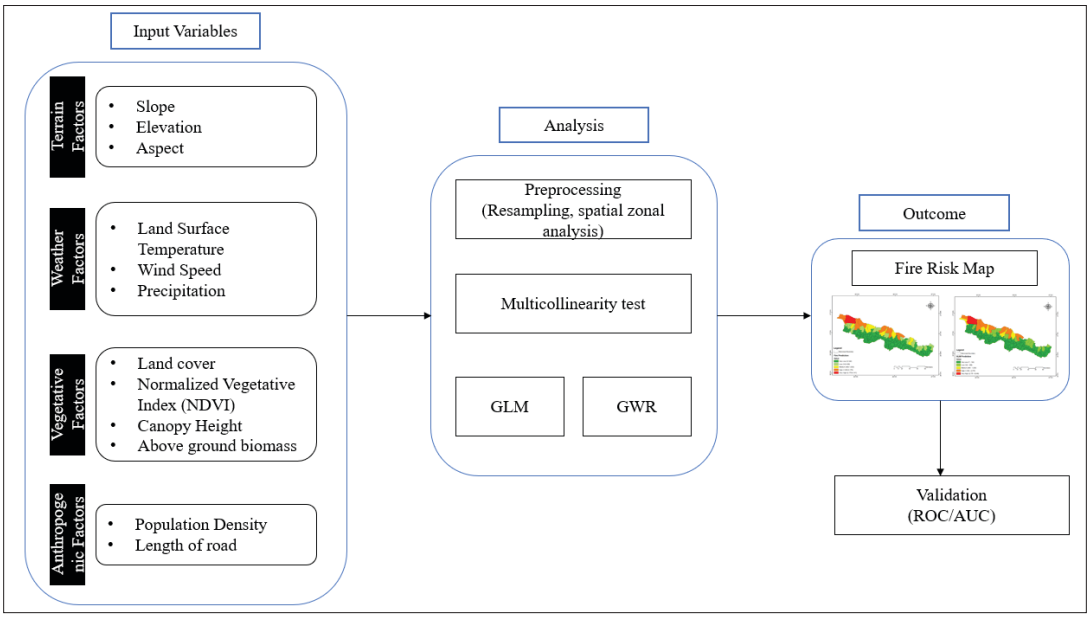

Figure 2: Methodological framework of the research

RESULTS

Trend of forest fire in Madhesh Province

Between 2012 and 2023, Madhesh Province experienced a significant number of fire incidents, with a total of 27,594 cases, resulting in a cumulative burnt area of 3460.52 km^2. On an annual average, the province experienced approximately 2299 fire incidents and a burnt area of 288.38 km^2. 2021 was the peak year for fire incidents, with a staggering 3743 cases, closely followed by 2016, which recorded 3406 incidents. In addition, 2021 recorded the highest burnt area, reaching 465.23 km^2, while 2014 ranked just behind with 461.31 km^2 (Figure 3). These statistics highlight the substantial impact and variability of fire incidents and burnt area within Madhesh Province over the study period. These findings emphasise the significant impact of fire occurrences on the affected areas. The data shown in Figure 3 offer valuable insights into the changing patterns of burnt area and fire incidence over the years.

Forest fire driving variables

The GLM model showed that 11 variables were significant (Appendix Table 2), with only the built-up area being insignificant. In contrast, the GWR model demonstrated significant results for variables that varied according to the features. Figure 4 illustrates the estimates of forest fire driving variables for both the GLM and GWR models. Several variables, including Aspect, Canopy Height, LST, rangeland area, agricultural area, and NDVI, showed positive estimates in both models. Windspeed was consistently negative across both GLM and GWR. However, Population Density exhibited a positive relationship in the GLM but a negative one in GWR, while Road Length was negative in the GLM but positive in the GWR. Notably, the forest area showed a positive estimated value

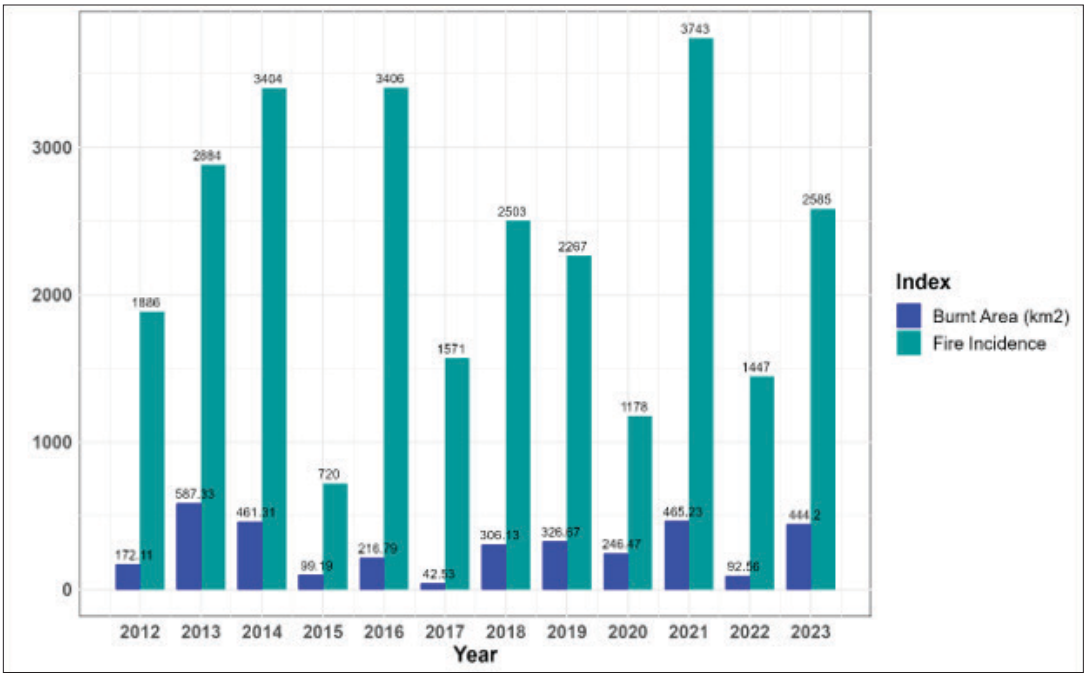

Figure 3: Forest fire incidents and burnt area in Madhesh province.

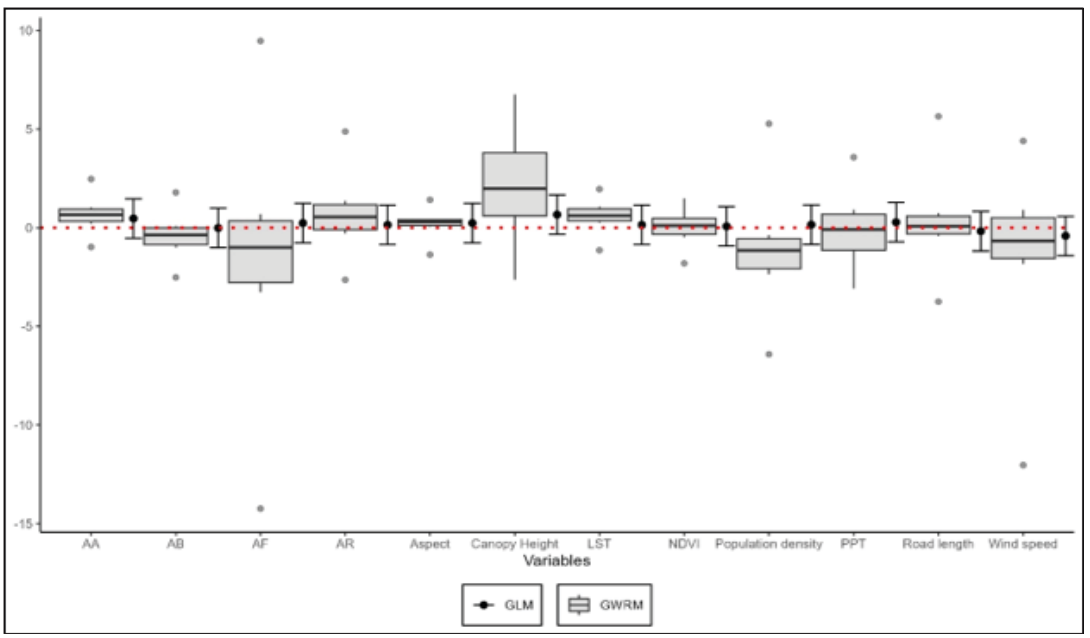

Figure 4: Estimates for forest fire driving variables from GLM and GWR model

in the GLM, whereas in the GWR model, despite a mean estimated value of -1.315, it took on both positive and negative values depending on the region, reflecting spatial variability.

To analyse the spatial non-stationarity of the variables in the GWR, a spatial mapping of the estimates was conducted. Additionally, to identify the significance of each variable, t-test values were calculated at a 5% level of significance. Based on these test values, municipalities were categorised as either significant or insignificant, with the results illustrated in the spatial map (Figure 5).

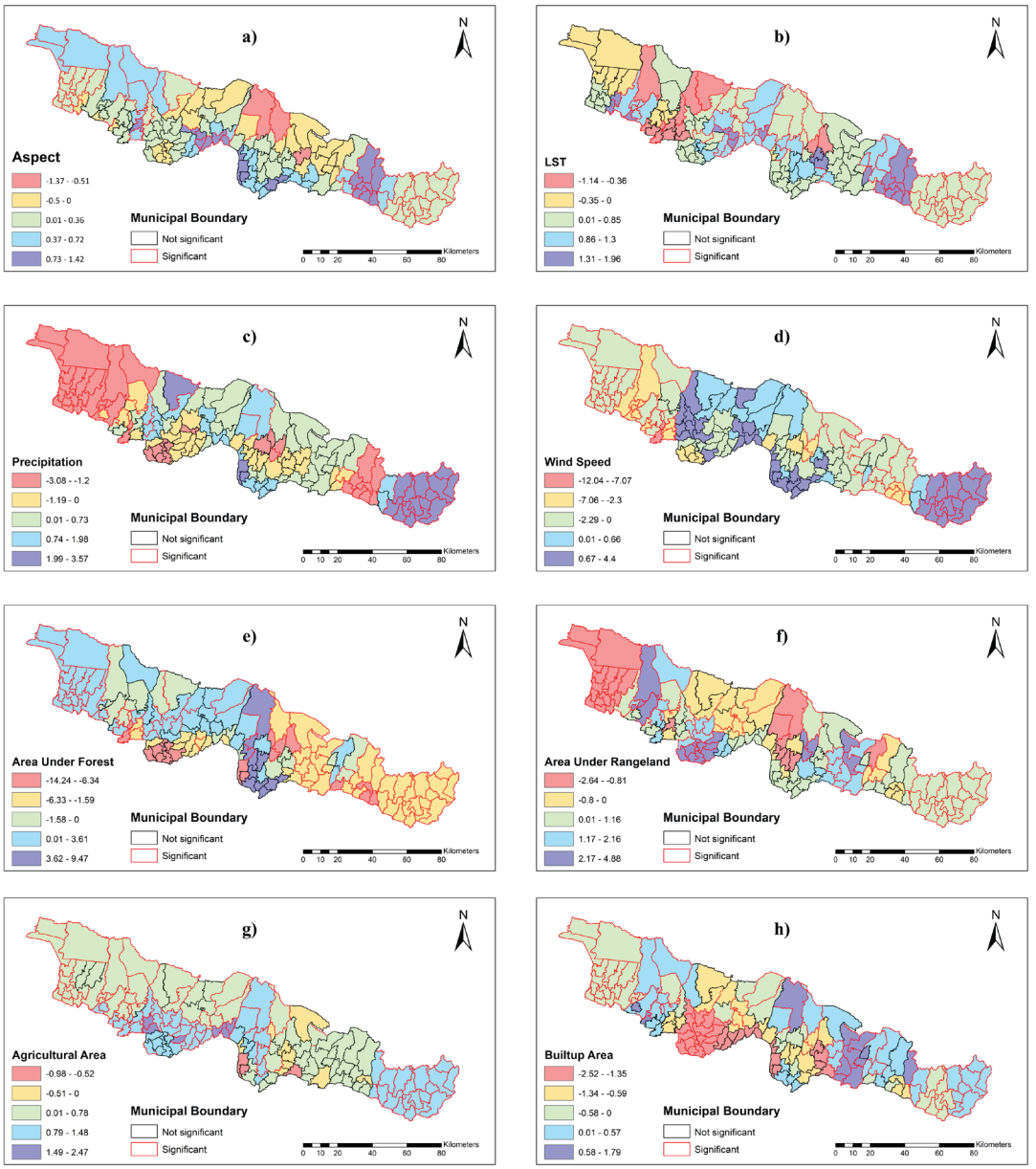

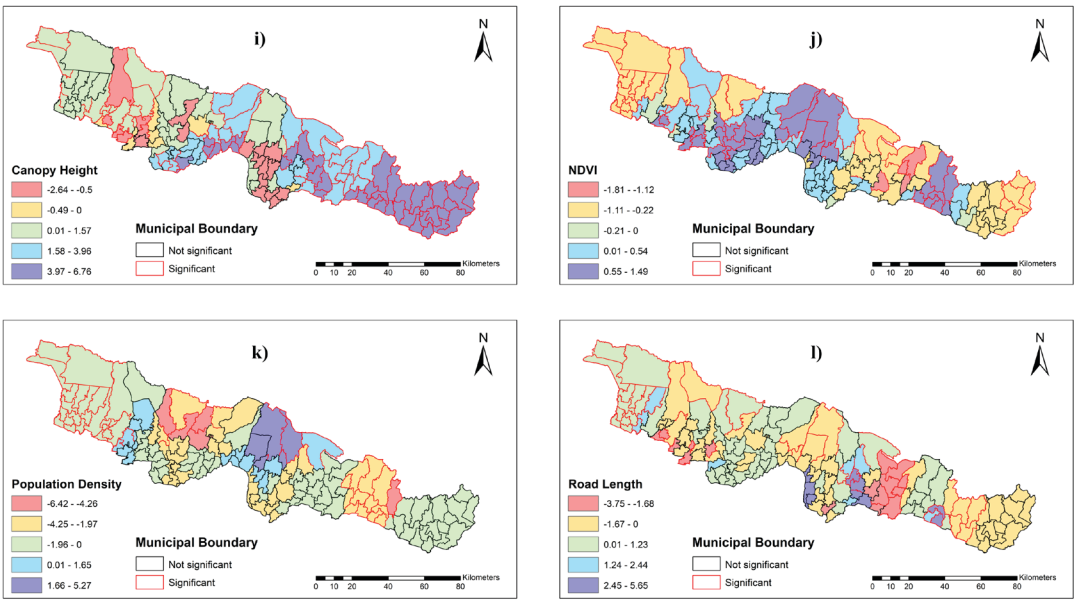

Figure 5: Spatial distribution of GWR estimates with significant (red outline) and insignificant municipalities (black outline): a) Aspect, b) Land surface temperature, c) Precipitation, d) Wind speed, e) Forest area, f) Rangeland area, g) Agricultural area, h) Built-up area, i) Canopy height, j) NDVI, k) Population density and l) Road length

Forest fire occurrence prediction map

The model used the variables and generated a final predicted map of forest fire occurrence, as shown in Figure 6. To depict the risk levels across the area, the predicted number of fire incidents was classified into five distinct risk categories. As illustrated in Table 3 and Figure 6, a clear difference in the predictions of the two models is apparent. The GWR model predicted a larger area of low and medium risk, whereas the GLM model predicted a larger area of very low risk (52.73%) compared to the GWR model (50.18%), indicating that the GLM tends to classify more areas as lower risk. Interestingly, both models predicted a similar high-risk area, with over 6000 fire incidents (Figure 6), is located in a protected national park. Other differences in the risk area suggest that GWR may capture local variations in fire risk more effectively, especially in the low to medium risk categories.

Table 3: Fire risk area Madhesh province

	GLM area (sq. km)	GWR area (sq. km)	GLM % Of risk area	GWR % Of risk area
Very low	5098	4846	52.77	50.18
Low	1486	1654	15.38	16.88
Medium	798	1012	8.26	10.53
High	1804	1674	18.67	17.45
Very High	475	475	4.92	4.96
Total	9661	9661	100.00	100.00

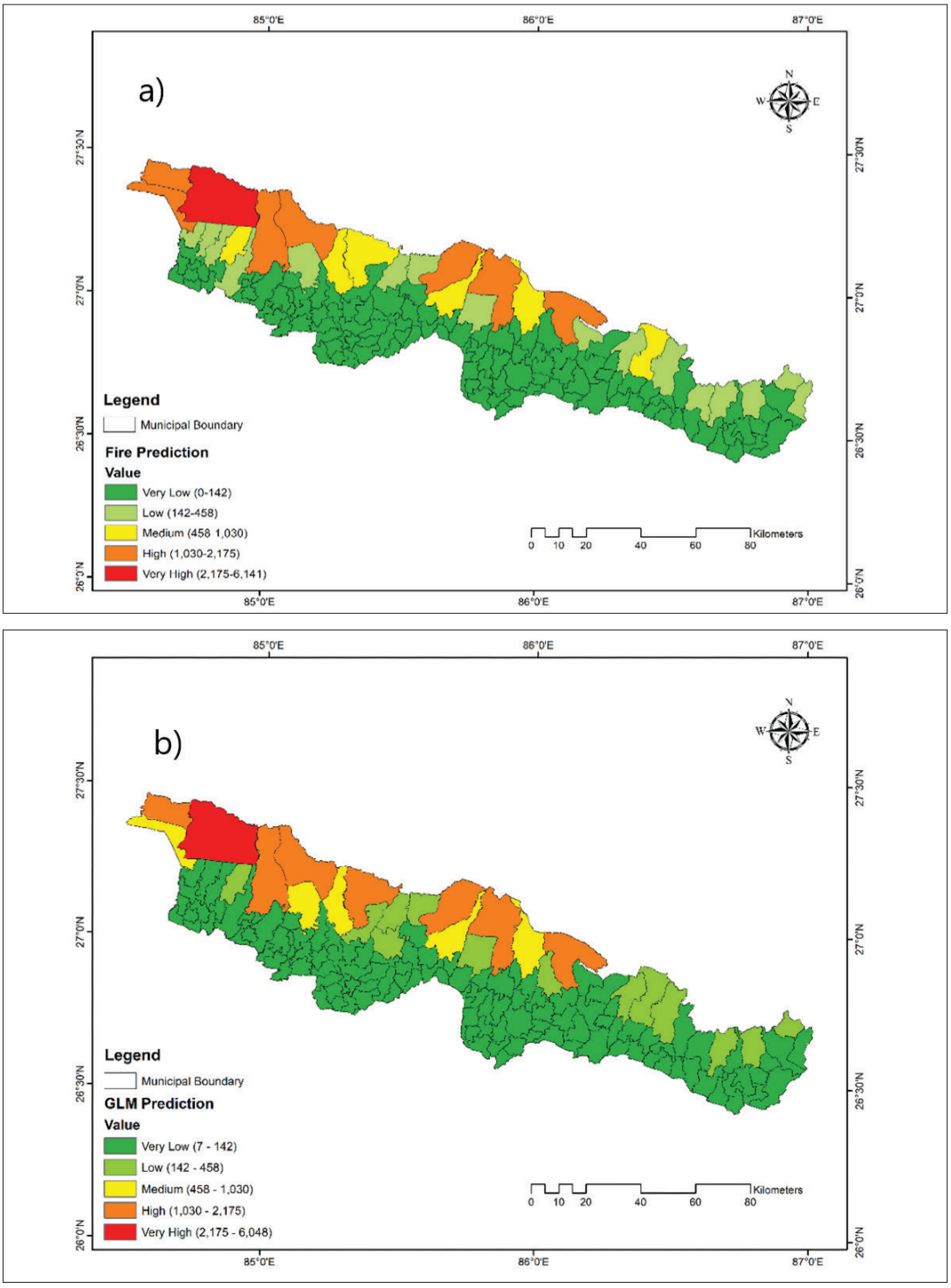

Figure 6: Fire occurrence prediction map of Madhesh province a) GWR model b) GLM model

Model diagnostic and validation

Model diagnostic results show that both the local and global models explained the variation very well. The global model assuming spatial homogeneity explains approximately 91.3 per cent of the variability in the response variable which is increased to 99.4 per cent by the local model utilising spatial heterogeneity of GWR. Moreover, the model shows a 92.7 per cent improvement when using local models instead of global models. The low AICc value of 942.849 also confirms the adequacy of the model fit, indicating its ability to balance goodness-of-fit and complexity for GWR.

Table 4: Model diagnostic for global (GLM) and local (GWR) model

Deviance explained by the global model (non-spatial)	0.913
Deviance explained by the local model	0.994
Deviance explained by the local model vs global model	0.927
AICc	942.849
Effective Degrees of Freedom	142.638
Adjusted Critical Value of Pseudo-t Statistics	2.665

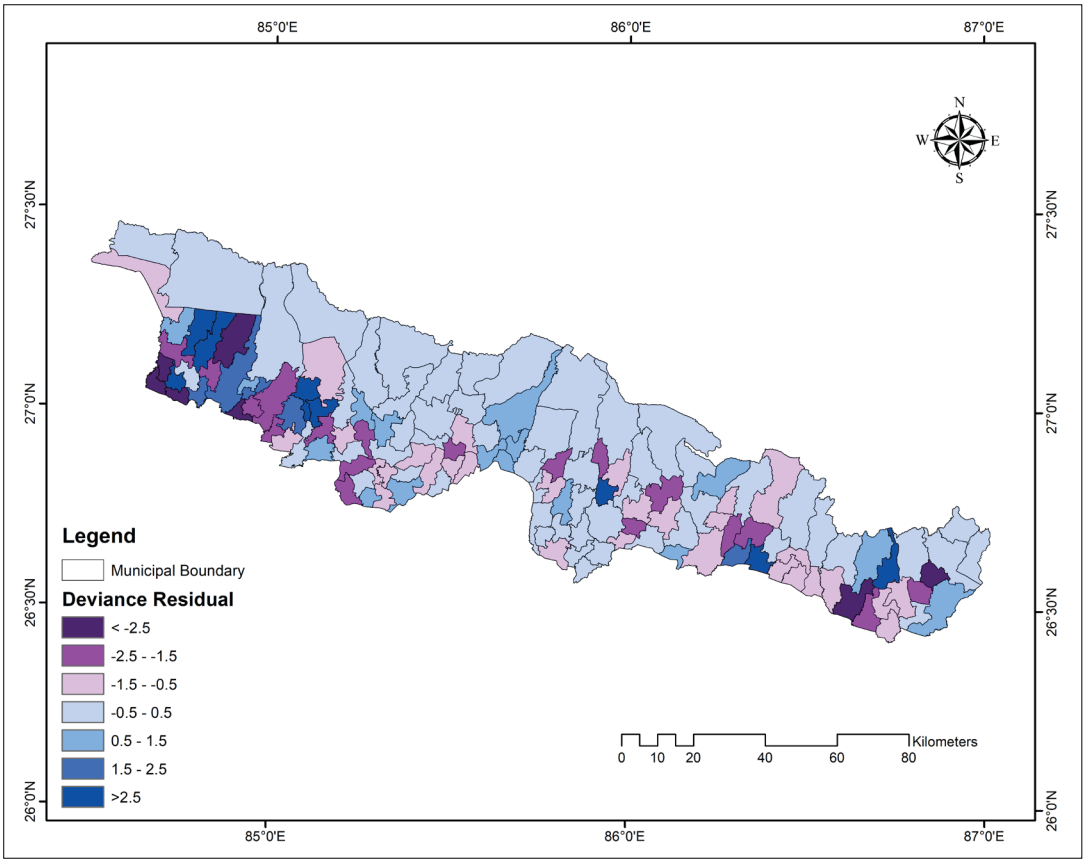

Figure 7: Map showing residual values across various municipal level from GWR model

Figure 7 displays the deviance residual map, illustrating the residual values across various municipal levels for GWR. In order to enhance the model and examine any potential clustering of the residuals, Moran's Index was employed for this study. The test results indicate that the pattern of residuals does not exhibit statistically significant spatial clustering. Therefore, it is interpreted as a random pattern.

In addition, using ROC method, we obtained an AUC value of 0.825 for GWR, which corresponds to an accuracy rate of 82.5 per cent. But the GLM performed poorly compared to GWR with an AUC value of 0.769. This outcome indicates that the results produced by the prediction map are deemed accurate based on the evaluation performed.

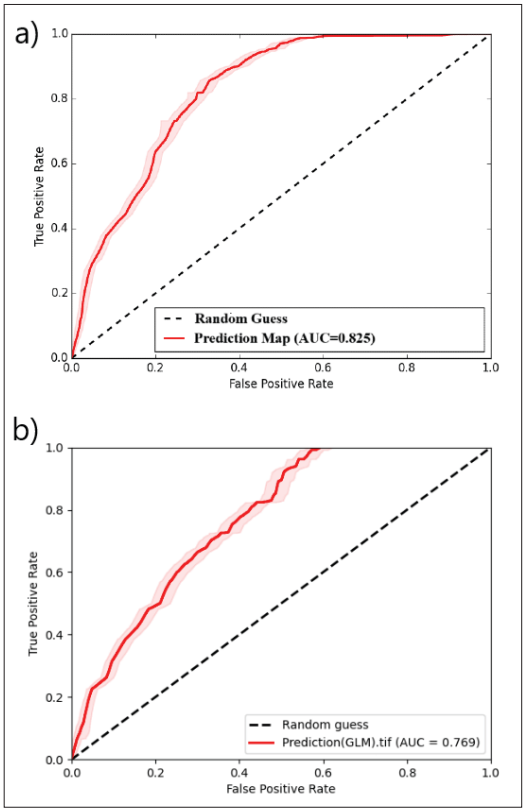

Figure 8: ROC/AUC of prediction map a) GWR model b) GLM model

DISCUSSION

Variable influence and spatial heterogeneity

Throughout the 12-year period, the burnt area fluctuated, with some years experiencing heightened destruction, while others saw a reduction. These fluctuations in burnt area and fire incidence demonstrate the unpredictable nature of fire occurrences. They also highlight the need for effective fire management and prevention strategies to mitigate the devastating impact of fires on the environment, ecosystems, and human lives. The effect of different drivers is discussed below.

Vegetation

In this study, the vegetation layers- forest area, rangeland, agriculture, NDVI and canopy height were used. All the variables revealed positive relations with both GLM and GWR models, but forest area showed a negative relationship with the GWR model. The study by Joshi *et al.* (2024), using a GLM model in the Chure region of Nepal, showed that an increase forest area was associated with a higher probability of fire occurrence, likely due to greater fuel availability in larger forested areas. While this trend is evident in our GLM results, the model does not capture spatial heterogeneity. The GWR model estimates for forest area ranged from 9.472 to -14.240 with an average estimate of -1.315 showing negative influence overall (Figure 5). The negative impact was observed in municipalities lying in the southern part dominated by agricultural zones. In the GLM, NDVI showed a positive relationship with forest fires, consistent with the results of Quan *et al.* (2022). However, the GWR results suggest a more nuanced, spatially

varying relationship. Areas with lower NDVI values, often indicative of vegetation under stress, such as drought conditions or sparse cover, were more susceptible to forest fires, likely because drier vegetation has lower resilience to ignition and fire spread (Chuvieco *et al.*, 2010), as illustrated in Figure 5(j). In addition, the province's forest consists of both deciduous species, such as Sal (*Shorea robusta*), and evergreen species, such as Sissoo (*Dalbergia sissoo*). Deciduous species shed their leaves seasonally, which reduces NDVI values and increases the risk of ground fires, as the accumulation of dry leaf litter on the forest floor provides abundant fuel (Aryal *et al.*, 2017).

For canopy height and rangeland positive estimates were observed in both models. Similar results for fire susceptibility in rangeland were also observed in the study of Joshi *et al.* (2024). Notably, canopy height had the highest average estimate value (0.66) and (2.04) for GLM and GWR respectively, among all the variables. Estimates of these variables also differed from -0.836 to 5.067, with most of the negative estimates concentrated in the western part of the province, pre-dominated by the protected area (Figure 5i). Interestingly, the canopy height distribution is also higher in the west and lower in the east of the province. This may indicate the possibility of ground fire being more prevalent but further research would be required to confirm it.

Climate and topography

As for climatic variables, LST displayed a significant and positive correlation with forest fire occurrences for both the GLM and GWR models. This finding aligns with previous research conducted by Guo *et al.* (2016) and Jolly *et al.* (2015). Summer temperatures in Madhesh province ranges from 32-38 degree Celsius (Fick and Hijmans, 2017). Higher surface temperatures lead to increased evapotranspiration conditions in trees, making the forest understory dry and more vulnerable (Li *et al.*, 2022) which in turn increases the probability of forest fires. In the case of precipitation, the GLM shows a positive relationship with forest fire occurrence. However, the GWR model reveals spatial variability, with a positive association towards the eastern part of the study area and a more negative influence of the variable in western region. In terms of topography, Madhesh province comprises Bhabhar, Dun Valley, and Chure in the north, which serve as sources of numerous rivulets and springs. Overall, occasional precipitation has been shown to reduce forest fire occurrence in Nepal (Bhujel *et al.*, 2017), whereas fire activity tends to increase in drier regions (Lafon and Quiring, 2012). However, areas with high precipitation and abundant fuel loads may also be susceptible to fire (Verhoeven *et al.*, 2020), while low precipitation can increase chances of drought and dry fuels, facilitating rapid spread of fire (Janizadeh *et al.*, 2023). Since the eastern region receives more rainfall than the western region (Mishra *et al.*, 2023), the GWR model is better at capturing this spatial heterogeneity than the GLM model. Although the effect of aspect was found to be significant by the GLM model, the GWR results reveal spatial variability, showing a positive relationship in the southwestern regions and a negative relationship in other areas, indicating that north-facing slopes may be more susceptible to fire. The study by Li *et al.* (2022), using the GWR model, suggests a similar trend at the global spatial scale. Furthermore, higher wind speeds can transport moist air from nearby water bodies, increasing humidity and reducing vegetation susceptibility to ignition.

This likely explains the predominantly negative relationship between wind speed and forest fire occurrence observed across a big part of the study area.

Anthropogenic drivers

In this analysis, key anthropogenic factors including population density, built-up area, and road length were considered. The GLM indicates a uniformly positive impact of population density, while road length and built-up area were not found to be significant. Fires near residential areas are often actively managed and supressed by locals, which may explain why anthropogenic variables are often found to be less influential (Mishra *et al.*, 2023). In contrast, the GWR shows clear spatial variability in these associations. All these variables show negative relationships in the southern, densely populated regions (Figure 5), but positive relationships in the more forest dominated areas, particularly in the Chure region of the province. This supports the findings of Hussin *et al.* (2008), indicating that fire-setting activities are more likely to occur farther from settlements.

Forest governance mechanisms

The forests of Madhesh are managed under the community forest program, and local communities depend on these resources to meet their daily needs, including fodder, fuelwood and timber (Shah *et al.*, 2022). Furthermore, to ensure the sound growth of yield, silvicultural management practices (weeding, thinning, pruning, controlled burning, etc.) are routinely implemented, resulting in a regular outflow of forest biomass (Dahal and Cao, 2017). Community forest user groups (CFUGs) and divisional forest offices (DFOs) are also pro-actively engaged in protecting these forests from fire, which helps to explain the negative relationship observed in some areas. However, as shown in Figure 5 (e), a positive relationship exists in the western part of Madhesh province. This region pre-dominantly falls under the protected area regime, including Parsa National Park, which covers an area of 637.37 sq. km (DNPWC, 2019). Under the National Parks and Wildlife Conservation Act of 1974, the collection or removal of any forest vegetation is prohibited in protected areas. Consequently, the accumulation of biomass in these regions can increase fire susceptibility during the dry season, explaining the positive relationship shown by the GWR model. In the context of agricultural areas (AA) there was a strong positive correlation with fire risk in both models. This aligns with the findings of Saikawa *et al.* (2020), who reported that the increasing prevalence of agricultural residue burning contributed to the spread of fire into adjacent forested areas.

Predictive model performance of GLM and GWR

Both the GLM and GWR models were used to predict the number of forest fires for the final forecast. Previous studies on the forest fire risk in Nepal have consistently identified the Terai Arc Landscape (TAL) region as the area with the highest risk (Parajuli *et al.*, 2020; Qadir *et al.*, 2021). Our research aligns with these findings and highlights a similar vulnerability in the Madhesh province. For validation the AUC value for both models was calculated. Figure 8 shows that the AUC value of the prediction map developed using GWR (AUC=0.825) is higher than that of the GLM (AUC=0.765), indicating the higher efficiency of the local model over the global model. Our findings are consistent with Cao *et al.* (2021), who showed that the GWR model provides a better fit than global models, producing more realistic spatial distributions

of forest fires. In our study, the GWR model also explains higher deviance than global GLM model. We considered the possibility of overfitting, however, the improved AICc, lack of spatial autocorrelation in residuals, and increased ROC/AUC values from independent validation indicate that GWR inherently retains the spatial heterogeneity. Moreover, the prediction maps generated by GWR closely resemble those from the GLM at the administrative unit level, but provide greater spatial detail, demonstrating that GWR refines the global model rather than contradicting it. This approach facilitates the development of tailored strategies for different municipalities, enabling more effective measures against forest fires. Future studies on spatial prediction of forest fires need to consider the heterogeneity in scales among different drivers (Li *et al.*, 2022).

Management and livelihood implications

The fire occurrence prediction map (Figure 6) clearly indicates the municipalities that are at higher risk of forest fires. Municipal government, forest department and other relevant agencies can use these findings to reduce damage to forest resources and minimise risks to the livelihoods of people dependent them. The DFOs and CFUGs can strategically adapt and implement fire lines in higher risk areas, with targeted efforts to segregate forest from settlement zones (Bhujel *et al.*, 2022). Similarly, several studies in the Asian context recommend the use of controlled burning in high-risk areas to reduce fuel loads and lower the potential intensity of fires during seasonal peaks (Parajuli *et al.*, 2022, Wang *et al.*, 2023). The models used in this study indicate that around 22 per cent of Madhesh province falls under high risk of fire, although the drivers vary spatially. Provincial and municipal governments can use this information to allocate site specific resources and budgets during their annual planning. Priority measures could include awareness programs, distribution of firefighting equipment and tools, and insurance policies for staff involved in fire risk management, strategies that have proven to be effective at the community level (Parajuli *et al.*, 2022). This research categorised municipalities according to their level of fire risk, enabling the prioritisation of targeted awareness programs and the implementation of early warning systems based on risk levels. SMS alerts, drill simulations and school/community awareness programs are for example some common early warning practices prevalent in south Asian context (Shah *et al.*, 2023). The province includes both, community forests which are governed and utilised to meet productive requirements of forest dependent livelihoods, and protected areas (Parsa National Park), conserved and managed for biodiversity protection. The municipal-scale fire risk prediction maps developed in this study can support Madhesh province in allocating and justifying resources for fire control across both protected and productive forest areas.

LIMITATIONS

The study provides insights on spatial drivers of forest fires and the non-stationary nature of these variables. While we studied the long-term patterns from 2012-2022, it does not explicitly account for short-term variations in climatic drivers, land-use practices, or fire management interventions. Future studies incorporating seasonal modelling frameworks could provide additional insights into these dynamics. Also, the inclusion of additional variables, like fuel moisture content, lightning-induced ignitions, and

controlled burning practices could further enhance the prediction of risk maps. As GWR estimates spatially varying parameters, model complexity increases relative to the number of observations. Although bandwidth selection and diagnostic checks were used to mitigate overfitting in this study, some degree of uncertainty may remain in local estimates, warranting cautious interpretation and more detailed studies.

CONCLUSION

The forest fire drivers in Madhesh province exhibited non stationery characteristics varying significantly on a spatial scale. We used both GLM and GWR models to predict forest fire scenarios, with the GWR model outperforming the GLM model, as indicated by the AIC values and AUC curves. The analysis demonstrates that aspect, LST, rangeland and agricultural area, canopy height, and NDVI values are positively related with fire risk, whereas precipitation, wind, vegetation coverage, and built-up area exhibit negative associations. The resulting prediction map indicates that around 22 per cent of Madhesh is exposed to high fire risk.

These insights have important implications for forest fire management planning. We recommend that GWR-based risk maps be used to guide local governmental and institutional bodies in designing context-specific interventions, such as directing controlled burning practices, building fire lines in high-risk zones, etc. Policymakers in the lowland regions of Nepal can integrate these highresolution risk maps into provincial land-use planning and community forest operational plans (CFOPs), as well as use them to allocate firefighting resources based on local needs, thereby enhancing preparedness and strengthening the resilience of local communities. For future research, we recommend incorporating socio-institutional variables (e.g., governance, law enforcement, community forest user group capacity, etc.) to better capture the human dimensions of fire risk. In addition, developing models that incorporate climate change scenarios would allow assessment of how shifting temperature and precipitation regimes may alter the spatial distribution of fire-prone zones over time.

Funding: The authors received no specific funding for this work

Competing interests: The authors have declared that no competing interests exist.

Declaration on AI-assisted technologies: AI-assisted tools were used only for language editing and improvement of sentence structure during manuscript preparation. The authors take full responsibility for the content of the manuscript.

REFERENCES

Adhikari, G., Joshi, K. P., Chand, D., Ghimire, A., & Mahara, S. (2025). Spatial dynamics and risk mapping of forest fires in Madhesh Province, Nepal: A multi-criteria decision approach. *Journal of Environment and Natural Resources, 23*(1), 80–94. https://doi.org/10.32526/ennrj/23/20240124

Aponte, C., De Groot, W. J., & Wotton, B. M. (2016). Forest fires and climate change: Causes, consequences and management options. *International Journal of Wildland Fire, 25*(8), i–ii. https://doi.org/10.1071/WFv25n8-FO

Aryal, B., Bhattarai, B. P., Pandey, M., & Devkota, S. (2017). Carbon sequestration in a fired ecosystem of Pinus roxburghii forest in Rasuwa District, Nepal. *Tropical Plant Research, 4*(2), 297–306. https://doi.org/10.22271/tpr.2017.v4.i2.039

Bajracharya, K. (2002). Forest fire situation in Nepal. *International Forest Fire News, 26*, 84–86.

Bhattarai, N., Dahal, S., Thapa, S., Pradhananga, S., Karky, B. S., Rawat, R. S., Windhorst, K., Watanabe, T., Thapa, R. B., & Avtar, R. (2022). Forest fire in the Hindu Kush Himalayas: A major challenge for climate action. *Journal of Forest and Livelihood, 21*(1), 14–31.

Bhujel, K. B., Maskey-Byanju, R., & Gautam, A. P. (2017). Wildfire dynamics in Nepal from 2000–2016. *Nepal Journal of Environmental Science, 5*, 1–8. https://doi.org/10.3126/njes.v5i0.22709

Bhujel, K., Sapkota, R., & Khadka, U. (2022). Temporal and spatial distribution of forest fires and their environmental and socio-economic implications in Nepal. *Journal of Forest and Livelihood, 21*(1), 1–13. https://doi.org/10.3126/jfl.v21i1.56575

Brunsdon, C., Fotheringham, A. S., & Charlton, M. E. (1996). Geographically weighted regression: A method for exploring spatial nonstationarity. *Geographical Analysis, 28*(4), 281–298. https://doi.org/10.1111/j.1538-4632.1996.tb00936.x

Cao, Q., Zhang, L., Su, Z., Wang, G., Sun, S., & Guo, F. (2021). Comparing four regression techniques to explore factors governing the number of forest fires in Southeast China. *Geomatics, Natural Hazards and Risk, 12*(1), 499–521. https://doi.org/10.1080/19475705.2021.1884609

Cardille, J. A., Ventura, S. J., & Turner, M. G. (2001). Environmental and social factors influencing wildfires in the Upper Midwest, United States. *Ecological Applications, 11*(1), 111–127. https://doi.org/10.1890/1051-0761(2001)011[0111:EASFIW]2.0.CO;2

Charlton, M., Fotheringham, A. S., & Brunsdon, C. (2009). *Geographically weighted regression.* National Centre for Geocomputation, National University of Ireland Maynooth.

Chatterjee, S., & Hadi, A. S. (2015). *Regression analysis by example.* John Wiley & Sons. https://doi.org/10.1002/0470055464.ch4

Chen, W., Qian, L., Shi, J., & Franklin, M. (2018). Comparing performance between log-binomial and robust Poisson regression models for estimating risk ratios under model misspecification. *BMC Medical Research Methodology, 18*(1), 63. https://doi.org/10.1186/s12874-018-0519-5

Chen, Y., Hall, J., van Wees, D., Andela, N., Hantson, S., Giglio, L., van der Werf, G. R., Morton, D. C., & Randerson, J. T. (2023). Multi-decadal trends and variability in burned area from the fifth version of the Global Fire Emissions Database (GFED5). *Earth System Science Data, 15*, 5227–5259. https://doi.org/10.5194/essd-15-5227-2023

Chuvieco, E., Aguado, I., Yebra, M., Nieto, H., Salas, J., Martín, M. P., Vilar, L., Martínez, J., Martín, S., Ibarra, P., de la Riva, J., Baeza, J., Rodríguez, F., Molina, J. R., Herrera, M. A., & Zamora, R. (2010). Development of a framework for fire risk assessment using remote sensing and geographic information system technologies. *Ecological Modelling, 221*(1), 46–58. https://doi.org/10.1016/j.ecolmodel.2008.11.017

CIESIN. (2018). *Gridded Population of the World, Version 4 (GPWv4): Population density, revision 11.* NASA Earthdata.

Comber, A., Brunsdon, C., Charlton, M., Dong, G., Harris, R., Lu, B., Lu, Y., Murakami, D., Nakaya, T., Wang, Y., & Harris, P. (2023). A route map for successful applications of geographically weighted regression. *Geographical Analysis, 55*(1), 155–178. https://doi.org/10.1111/gean.12316

Coskuner, K. A. (2022). Assessing the performance of MODIS and VIIRS active fire products in the monitoring of wildfires: A case study in Turkey. *iForest: Biogeosciences and Forestry, 15*(2), 85–94. https://doi.org/10.3832/ifor3754-015

Dahal, D. S., & Cao, S. (2017). Sustainability assessment of community forestry practices in Nepal: Literature review and recommendations to improve community management. *Proceedings of the National Academy of Sciences, 87*(1), 1–11. https://doi.org/10.1007/s40011-015-0627-5

Devkota, M., Hatfield, G., & Chintala, R. (2014). Effect of sample size on the performance of ordinary least squares and geographically weighted regression. *British Journal of Mathematics & Computer Science, 4*(1), 1–21. https://doi.org/10.9734/BJMCS/2014/6050

Dhakal, M., Bhatta, B., Lamichhane, P., & Parajuli, A. (2024). Synergistic approaches in forest fire risk mapping using fuzzy AHP and machine learning models in the Chure Tarai Madhesh Landscape (CTML) of Nepal. *Geomatics, Natural Hazards and Risk, 15*(1), 2436540. https://doi.org/10.1080/19475705.2024.2436540

Department of National Parks and Wildlife Conservation. (2019). *Parsa National Park.* https://dnpwc.gov.np/protected_areas/details/parsawildlifereserve

Environmental Systems Research Institute. (2022). *ArcGIS Pro (Version 3.0)* [Software]. https://www.esri.com/

Fick, S. E., & Hijmans, R. J. (2017). WorldClim 2: New 1-km spatial resolution climate surfaces for global land areas. *International Journal of Climatology, 37*(12), 4302–4315. https://doi.org/10.1002/joc.5086

Flach, P. A. (2016). ROC analysis. In C. Sammut & G. I. Webb (Eds.), *Encyclopedia of machine learning and data mining* (pp. 1–8). Springer. https://doi.org/10.1007/978-1-4899-7502-7_739-1

Ganteaume, A., Camia, A., Jappiot, M., San-Miguel-Ayanz, J., Long-Fournel, M., & Lampin, C. (2013). A review of the main driving factors of forest fire ignition over Europe. *Environmental Management, 51*(3), 651–662. https://doi.org/10.1007/s00267-012-9961-z

Giglio, L., Schroeder, W., & Hall, J. V. (2020). *MODIS collection 6 active fire product user's guide revision C.* NASA.

Giglio, L., van der Werf, G. R., Randerson, J. T., Collatz, G. J., & Kasibhatla, P. (2006). Global estimation of burned area using MODIS active fire observations. *Atmospheric Chemistry and Physics, 6*(4), 957–974. https://doi.org/10.5194/acp-6-957-2006

Guo, F., Wang, G., Su, Z., Liang, H., Wang, W., Lin, F., & Liu, A. (2016). What drives forest fire in Fujian, China? Evidence from logistic regression and random forests. *International Journal of Wildland Fire, 25*(5), 505–519. https://doi.org/10.1071/WF15121

Hussin, Y. A., Matakala, M., & Zagdaa, N. (2008). The applications of remote sensing and GIS in modeling forest fire hazard in Mongolia. In *XXI ISPRS Congress 2008: Silk Road for Information from Imagery.*

İnan, M., Bilici, E., & Akay, A. E. (2017). Using airborne LiDAR data for assessment of forest fire fuel load potential. *ISPRS Annals of the Photogrammetry, Remote Sensing and Spatial Information Sciences, IV-4/W4*, 255–258. https://doi.org/10.5194/isprs-annals-IV-4-W4-255-2017

Janizadeh, S., Bateni, S. M., Jun, C., Im, J., Pai, H. T., Band, S. S., & Mosavi, A. (2023). Combination four different ensemble algorithms with the generalized linear model (GLM) for predicting forest fire susceptibility. *Geomatics, Natural Hazards and Risk, 14*(1), 2206512. https://doi.org/10.1080/19475705.2023.2206512

Jolly, W. M., Cochrane, M. A., Freeborn, P. H., Holden, Z. A., Brown, T. J., Williamson, G. J., & Bowman, D. M. J. S. (2015). Climate-induced variations in global wildfire danger from 1979 to 2013. *Nature Communications, 6*(1), 7537. https://doi.org/10.1038/ncomms8537

Joshi, K. P., Adhikari, G., Bhattarai, D., Adhikari, A., & Lamichhane, S. (2024). Forest fire vulnerability in Nepal's Chure region: Investigating the influencing factors using generalized linear model. *Heliyon, 10*(7), e28525. https://doi.org/10.1016/j.heliyon.2024.e28525

Kolanek, A., Szymanowski, M., & Raczyk, A. (2021). Human activity affects forest fires: The impact of anthropogenic factors on the density of forest fires in Poland. *Forests, 12*(6), Article 728. https://doi.org/10.3390/f12060728

Koutsias, N., Martínez-Fernández, J., & Allgöwer, B. (2010). Do factors causing wildfires vary in space? Evidence from geographically weighted regression. *GIScience & Remote Sensing, 47*(2), 221–240. https://doi.org/10.2747/1548-1603.47.2.221

Lafon, C. W., & Quiring, S. M. (2012). Relationships of fire and precipitation regimes in temperate forests of the eastern United States. *Earth Interactions, 16*(11), 1–15. https://doi.org/10.1175/2012EI000442.1

Li, W., Xu, Q., Yi, J., & Liu, J. (2022). Predictive model of spatial scale of forest fire driving factors: A case study of Yunnan Province, China. *Scientific Reports, 12*(1), 19029. https://doi.org/10.1038/s41598-022-23697-6

Maingi, J. K., & Henry, M. C. (2007). Factors influencing wildfire occurrence and distribution in eastern Kentucky, USA. *International Journal of Wildland Fire, 16*(1), 23–33. https://doi.org/10.1071/WF06007

Martínez-Fernández, J., Chuvieco, E., & Koutsias, N. (2013). Modelling long-term fire occurrence factors in Spain by accounting for local variations with geographically weighted regression. *Natural Hazards and Earth System Sciences, 13*(2), 311–327. https://doi.org/10.5194/nhess-13-311-2013

Matin, M. A., Chitale, V. S., Murthy, M. S. R., Uddin, K., Bajracharya, B., & Pradhan, S. (2017). Understanding forest fire patterns and risk in Nepal using remote sensing, geographic information system and historical fire data. *International Journal of Wildland Fire, 26*(4), 276–286. https://doi.org/10.1071/WF16056

Mishra, B., Panthi, S., Poudel, S., & Ghimire, B. R. (2023). Forest fire pattern and vulnerability mapping using deep learning in Nepal. *Fire Ecology, 19*(1), 3. https://doi.org/10.1186/s42408-022-00162-3

Mullahy, J. (1986). Specification and testing of some modified count data models. *Journal of Econometrics, 33*(3), 341–365. https://doi.org/10.1016/0304-4076(86)90002-3

Myers, R. H., Montgomery, D. C., Vining, G. G., & Robinson, T. J. (2012). *Generalized linear models: With applications in engineering and the sciences.* John Wiley & Sons.

Parajuli, A., Gautam, A. P., Sharma, S. P., Bhujel, K. B., Sharma, G., Thapa, P. B., Bist, B. S., & Poudel, S. (2020). Forest fire risk mapping using GIS and remote sensing in two major landscapes of Nepal. *Geomatics, Natural Hazards and Risk, 11*(1), 2569–2586. https://doi.org/10.1080/19475705.2020.1853251

Parajuli, A., Gautam, A. P., Sharma, S., Lamichhane, P., Sharma, G., Bist, B., Aryal, U., & Basnet, R. (2022). A strategy for involving community forest managers in effective forest fire management in Nepal. *Banko Janakari, 32*(1), 41–51. https://doi.org/10.3126/banko.v32i1.45476

Parajuli, A., Manzoor, S. A., & Lukac, M. (2023). Areas of the Terai Arc landscape in Nepal at risk of forest fire identified by fuzzy analytic hierarchy process. *Environmental Development, 45*, 100810. https://doi.org/10.1016/j.envdev.2023.100810

Paudel, G., Pandey, K., Lamsal, P., Bhattarai, A., Bhattarai, A., & Tripathi, S. (2024). Geospatial forest fire risk assessment and zoning by integrating MaxEnt in Gorkha District, Nepal. *Heliyon, 10*(11), e31305. https://doi.org/10.1016/j.heliyon.2024.e31305

Piao, S., *et al.* (2018). Lower land-use emissions responsible for increased net land carbon sink during the slow warming period. *Nature Geoscience, 11*(10). https://doi.org/10.1038/s41561-018-0204-7

Posavec, S., Barčić, D., Vuletić, D., Vučetić, V., Čavlina Tomašević, I., & Pezdevšek Malovrh, Š. (2023). Forest fires, stakeholders' activities, and economic impact on state-level sustainable forest management. *Sustainability, 15*(22), 16080. https://doi.org/10.3390/su152216080

Qadir, A., Talukdar, N. R., Uddin, M. M., Ahmad, F., & Goparaju, L. (2021). Predicting forest fire using multispectral satellite measurements in Nepal. *Remote Sensing Applications: Society and Environment, 23*, 100539. https://doi.org/10.1016/j.rsase.2021.100539

Quan, D., Quan, H., Zhu, W., Lin, Z., & Jin, R. (2022). A comparative study on the drivers of forest fires in different countries in the cross-border area between China, North Korea and Russia. *Forests, 13*(11), Article 1939. https://doi.org/10.3390/f13111939

Robinne, F. N. (2021). *Impacts of disasters on forests, in particular forest fires.* United Nations Forum on Forests Secretariat.

Sá, A. C. L., Pereira, J. M. C., Charlton, M. E., Mota, B., Barbosa, P. M., & Fotheringham, A. S. (2011). The pyrogeography of sub-Saharan Africa: A study of the spatial non-stationarity of fire-environment relationships using GWR. *Journal of Geographical Systems, 13*(3), 227–248. https://doi.org/10.1007/s10109-010-0123-7

Saikawa, E., Wu, Q., Zhong, M., Avramov, A., Ram, K., Stone, E. A., Stockwell, C. E., Jayarathne, R., Panday, A. K., & Yokelson, R. J. (2020). Garbage burning in South Asia: How important is it to regional air quality? *Environmental Science & Technology, 54*(16), 9928–9938. https://doi.org/10.1021/acs.est.0c02830

Shah, A., Ullah, A., Khan, N., Khan, A., Tariq, M., & Xu, C. (2023). Community social barriers to non-technical aspects of flood early warning systems and NGO-led interventions: The case of Pakistan. *Frontiers in Earth Science, 11*. https://doi.org/10.3389/feart.2023.1068721

Shah, S., Gautam, N. P., Dhakal, B. P., Sah, J. N., & Sharma, S. C. (2022). Impact of land cover dynamics on ecosystem services value of Siwalik range of Madhesh Province Nepal. *International Journal of Agricultural and Applied Sciences, 3*(2), 94–99. https://doi.org/10.52804/ijaas2022.3217

Sharples, J. J. (2009). An overview of mountain meteorological effects relevant to fire behaviour and bushfire risk. *International Journal of Wildland Fire, 18*(7), 737–754. https://doi.org/10.1071/WF08041

Sofan, P., Bruce, D., Schroeder, W., Jones, E., & Marsden, J. (2020). Assessment of VIIRS 375 m active fire using tropical peatland combustion algorithm applied to Landsat-8 over Indonesia's peatlands. *International Journal of Digital Earth, 13*(12), 1695–1716. https://doi.org/10.1080/17538947.2020.1791268

Turco, M., Llasat, M. C., von Hardenberg, J., & Provenzale, A. (2013). Impact of climate variability on summer fires in a Mediterranean environment (northeastern Iberian Peninsula). *Climatic Change, 116*(3), 665–678. https://doi.org/10.1007/s10584-012-0505-6

Verhoeven, E. M., Murray, B. R., Dickman, C. R., Wardle, G. M., & Greenville, A. C. (2020). Fire and rain are one: Extreme rainfall events predict wildfire extent in an arid grassland. *International Journal of Wildland Fire, 29*(8), 702–711. https://doi.org/10.1071/WF19087

Wang, J., Hong, R., Ma, C., Zhu, X., Xu, S., Tang, Y., Li, X., Yan, X., Wang, L., & Wang, Q. (2023). Effects of prescribed burning on surface dead fuel and potential fire behavior in Pinus yunnanensis in Central Yunnan Province, China. *Forests, 14*(9), 1915. https://doi.org/10.3390/f14091915

Xiao, Y., Zhang, X., & Ji, P. (2015). Modeling forest fire occurrences using count-data mixed models in Qiannan Autonomous Prefecture of Guizhou Province in China. *PLOS ONE, 10*(3), e0120621. https://doi.org/10.1371/journal.pone.0120621

Yang, X., Jin, X., & Zhou, Y. (2021). Wildfire risk assessment and zoning by integrating MaxEnt and GIS in Hunan Province, China. *Forests, 12*(10), Article 1299. https://doi.org/10.3390/f12101299

Yu, S., Ye, Q., Zhao, Q., Li, Z., Zhang, M., Zhu, H., & Zhao, Z. (2022). Effects of driving factors on forest aboveground biomass (AGB) in China's Loess Plateau by using spatial regression models. *Remote Sensing, 14*(12), 2842. https://doi.org/10.3390/rs14122842

Zeng, G., & Tao, S. (2023). A generalized linear transformation and its effects on logistic regression. *Mathematics, 11*(2), 467. https://doi.org/10.3390/math11020467

Zhang, J.-H., Yao, F.-M., Liu, C., Yang, L.-M., & Boken, V. K. (2011). Detection, emission estimation and risk prediction of forest fires in China using satellite sensors and simulation models in the past three decades: An overview. *International Journal of Environmental Research and Public Health, 8*(8), 3156–3178. https://doi.org/10.3390/ijerph8083156